

See discussions, stats, and author profiles for this publication at: <https://www.researchgate.net/publication/239717678>

# Surface Characterization of $\gamma$ -Ga<sub>2</sub>O<sub>3</sub>: A Microcalorimetric and IR Spectroscopic Study of CO Adsorption

ARTICLE in LANGMUIR · DECEMBER 2002

Impact Factor: 4.46 · DOI: 10.1021/la026362x

CITATIONS

24

READS

8

5 AUTHORS, INCLUDING:



**Montserrat Rodríguez Delgado**

University of the Balearic Islands

64 PUBLICATIONS 1,315 CITATIONS

SEE PROFILE



**Claudio Morterra**

Università degli Studi di Torino

240 PUBLICATIONS 7,580 CITATIONS

SEE PROFILE



**Carlos Otero Areán**

University of the Balearic Islands

224 PUBLICATIONS 5,247 CITATIONS

SEE PROFILE

# Surface Characterization of $\gamma$ -Ga<sub>2</sub>O<sub>3</sub>: A Microcalorimetric and IR Spectroscopic Study of CO Adsorption

M. Rodríguez Delgado,<sup>†</sup> C. Morterra,<sup>\*,‡</sup> G. Cerrato,<sup>‡</sup> G. Magnacca,<sup>‡</sup> and C. Otero Areán<sup>†</sup>

*Departamento de Química, Universidad de las Islas Baleares, 07071 Palma de Mallorca, Spain, and Dipartimento di Chimica IFM, Università di Torino and Consorzio INSTM, Unità di Ricerca di Torino, 10125 Torino, Italy*

*Received August 6, 2002. In Final Form: October 16, 2002*

Strong Lewis acidity of a phase-pure  $\gamma$ -Ga<sub>2</sub>O<sub>3</sub> was studied by the adsorption of CO at ambient temperature, with the combined use of adsorption microcalorimetry and in situ Fourier transform infrared spectroscopy. The concentration of strong Lewis acid sites turned out to be quite low, but it grew fast with increasing surface dehydration upon thermal treatments in the 573–773 K range. Two main families of Lewis acid sites were observed, characterized by rather different molar adsorption heats and CO stretching frequencies. These acid sites have been ascribed to coordinatively unsaturated Ga<sup>3+</sup> ions located in defective (higher  $\nu_{\text{CO}}$ ) and regular (lower  $\nu_{\text{CO}}$ ) crystallographic sites, respectively. The possibility of extracting, for the CO/ $\gamma$ -Ga<sub>2</sub>O<sub>3</sub> system, quantitative information from the IR spectroscopic data is discussed in some detail.

## 1. Introduction

Gallium(III) oxide, also known as gallia, presents a polymorphism analogous to that of alumina.<sup>1</sup> The only thermodynamically stable polymorph is  $\beta$ -Ga<sub>2</sub>O<sub>3</sub>, which has a monoclinic structure. However, several metastable (low temperature) forms of Ga<sub>2</sub>O<sub>3</sub> exist, which are similar to the well-known *transition aluminas*,<sup>2</sup> depending on the preparation conditions, they can appear as single or as mixed crystal phases.<sup>3</sup> Among these metastable polymorphs,  $\gamma$ -Ga<sub>2</sub>O<sub>3</sub> has a defective spinel-type structure analogous to that of  $\gamma$ -Al<sub>2</sub>O<sub>3</sub>. Preparation of this polymorph as a pure crystalline phase has recently been reported,<sup>3</sup> as well as a preliminary characterization of its surface structure. The present work is aimed at a further and detailed study of the surface chemistry of phase-pure  $\gamma$ -Ga<sub>2</sub>O<sub>3</sub>, which is accomplished by using Fourier transform infrared (FTIR) spectroscopy and microcalorimetric measurements of adsorbed carbon monoxide.

Understanding of the surface chemistry of  $\gamma$ -Ga<sub>2</sub>O<sub>3</sub> is relevant in view of (i) the possible presence in the surface layers of  $\gamma$ -Ga<sub>2</sub>O<sub>3</sub> of both tetrahedral and octahedral cationic sites, which can be studied without the perturbations deriving from the presence of mixed phases; (ii) the use of gallium-containing materials (mainly zeolites) as industrial catalysts, for example, for hydrocarbon dehydrogenation and cyclization;<sup>4,5</sup> (iii) the recently claimed potential use of Ga-containing oxidic systems as catalysts

for the abatement of nitrogen oxides<sup>6</sup> and for hydrocarbon isomerization;<sup>7</sup> and (iv) the fact that in these catalytic processes both structural features and the role played by gallium surface centers are still far from being understood. The combined use of FTIR spectroscopy and adsorption microcalorimetry affords characterization of the strong Lewis acidity of  $\gamma$ -Ga<sub>2</sub>O<sub>3</sub>, that is, the acidic character of coordinatively unsaturated cations as monitored by interaction (at ambient temperature) with a weak Lewis base such as CO. FTIR spectroscopy of adsorbed CO gives information on the types of acidic sites present and on their relative proportions, while adsorption microcalorimetry helps to quantify the interaction energy and the amount of adsorbed CO.

## 2. Experimental Section

**2.1. Materials.** Phase-pure  $\gamma$ -Ga<sub>2</sub>O<sub>3</sub> was prepared starting from an ethanolic solution of high-purity (hydrated) gallium nitrate (Avocado Italia, s.r.l.) and concentrated aqueous ammonia diluted in ethanol, as described in detail elsewhere.<sup>3</sup> The hydrated gallia gel thus obtained was thoroughly washed, filtered, and vacuum-dried, and the resulting xerogel was calcined in air at 573 K (30 min) leading to a single-phase  $\gamma$ -Ga<sub>2</sub>O<sub>3</sub> polymorph having the spinel-type structure, as revealed by powder X-ray diffraction (XRD);<sup>3</sup> this material is hereafter referred to as the “starting  $\gamma$ -Ga<sub>2</sub>O<sub>3</sub>”. From N<sub>2</sub> adsorption–desorption isotherms at 77 K, the Brunauer–Emmett–Teller (BET) surface area of the starting  $\gamma$ -Ga<sub>2</sub>O<sub>3</sub> was found to be  $S_{\text{BET}} = 191 \text{ m}^2 \text{ g}^{-1}$ , and the pore volume  $V_p = 0.16 \text{ cm}^3 \text{ g}^{-1}$ , as reported in the first row of Table 1.

For both IR and microcalorimetric adsorption measurements,  $\gamma$ -Ga<sub>2</sub>O<sub>3</sub> required a proper in situ vacuum activation, which was carried out as follows. The starting  $\gamma$ -Ga<sub>2</sub>O<sub>3</sub> underwent a first activation in vacuo and oxidation (40 Torr O<sub>2</sub>) in the vacuum system at 673 K, to eliminate the impurities present on the sample (basically nitrates, carbonates, and carbonaceous residues, deriving from the early steps of preparation, calcination, and exposure to the atmosphere); this step was followed by a thorough rehydration (in the vacuum system, with saturated water vapor at ambient temperature) and a final in situ vacuum activation (2 h, residual pressure  $< 10^{-5}$  Torr) and oxygen treatment at one of the selected temperatures: 573, 673, and 773 K. The

\* Corresponding author. Prof. Claudio Morterra, Dipartimento di Chimica IFM, via P. Giuria 7, 10125 Torino, Italy. Tel: +39 011 670 7589. Fax: +39 011 670 7855. E-mail: claudio.morterra@unito.it.

<sup>†</sup> Universidad de las Islas Baleares.

<sup>‡</sup> Università di Torino and Consorzio INSTM.

(1) Greenwood, N. N.; Earnshaw, A. *Chemistry of the Elements*; Pergamon Press: Oxford, 1984.

(2) Lippens, B. C.; Steggerda, J. J. *Physical and Chemical Aspects of Adsorbents and Catalysts*; Linsen, B. G., Fortuin, M. H., Okkersee, C., Steggerda, J. J., Eds.; Academic Press: London, 1970; p 171.

(3) Otero Areán, C.; López Bellan, A.; Peñarroya Mentrut, M.; Rodríguez Delgado, M.; Turnes Palomino, G. *Microporous Mesoporous Mater.* **2000**, *40*, 35.

(4) Inui, T.; Matsuda, H.; Yamase, O.; Nagata, H.; Fukuda, K.; Ukawa, T.; Miyamoto, A. *J. Catal.* **1986**, *40*, 491.

(5) Khodakov, A. Yu.; Kustov, L. M.; Bondarenko, T. N.; Dergachev, A. A.; Kazansky, V. B.; Minachev, Kh. M.; Borbely, G.; Beyer, H. K. *Zeolites* **1990**, *10*, 603.

(6) Haneda, M.; Kintaichi, Y.; Hamada, H. *Appl. Catal., B* **1999**, *20*, 289.

(7) Moreno, J. A.; Poncelet, G. *J. Catal.* **2001**, *203*, 453.

**Table 1. BET Surface Area, Pore Volume, and Average Pore Radius for  $\gamma$ -Ga<sub>2</sub>O<sub>3</sub> Specimens (N<sub>2</sub> Adsorption/Desorption Isotherms at 77 K)**

sample	$S_{\text{BET}}$ (m <sup>2</sup> g <sup>-1</sup> )	$V_{\text{p}}$ (cm <sup>3</sup> g <sup>-1</sup> )	$R_{\text{p}}$ (nm)
starting $\gamma$ -Ga <sub>2</sub> O <sub>3</sub>	191	0.16	1.5
G573	163	0.19	2.0
G673	163	0.19	2.0
G773	142	0.16	1.8
G <sub>773</sub> 573	142	0.16	1.8

corresponding activated samples are hereafter referred to as G573, G673, and G773, respectively. The described treatments caused no structural modifications, as checked by powder X-ray diffraction, but some textural changes were observed as summarized in Table 1. Since the thermal treatment at the highest temperature caused, as expected, the onset of a partial sintering process, some of the G773 material was thoroughly rehydrated at ambient temperature and then underwent a second activation–oxidation cycle at 573 K leading to the sample termed G<sub>773</sub>573.

**2.2. Methods.** For FTIR study of CO adsorption, samples of the starting  $\gamma$ -Ga<sub>2</sub>O<sub>3</sub> were prepared in the form of thin self-supporting wafers ( $\sim 15$  mg cm<sup>-2</sup>) and transferred to a homemade quartz vacuum cell where they underwent all treatments (i.e., the described activation, CO adsorption and desorption, and eventual rehydration steps) in a strictly in situ configuration. FTIR spectra of CO adsorption/desorption were obtained at beam-temperature (BT) that is conventionally assumed to correspond to the ambient temperature but is actually likely to be (at least) some 20–30 K higher. All IR spectra were recorded at 2 cm<sup>-1</sup> resolution on a Bruker FTIR IFS 113v instrument, equipped with a MCT cryodetector. The roto-vibrational component due to gas-phase CO was interactively subtracted from the spectra of adsorbed CO. Spectral deconvolutions were carried out using the FIT routine by Bruker and adopting free and fixed parameters as stated further on.

On  $\gamma$ -Ga<sub>2</sub>O<sub>3</sub> samples prepared and activated as described above, microcalorimetric measurements were carried out at 303 K using a heat-flow microcalorimeter (standard Tian-Calvet type, Seratam, France) connected to a gas-volumetric apparatus which enabled the simultaneous determination of evolved heats (integral adsorption heats,  $Q_{\text{int}}$ ) and adsorbed amounts ( $N_{\text{a}}$ ). The two sets of experimental data, normalized per unit surface area, led to the calculation of molar adsorption heats ( $q^{\text{diff}}$ ). To check the possible presence of irreversible CO adsorption processes, on each sample the first adsorption run, up to a final equilibrium pressure of  $\sim 80$  Torr (primary isotherms), was followed by an overnight evacuation at ambient temperature and then by a second adsorption run up to the same final pressure (secondary isotherms). The possible presence of irreversible adsorption and/or surface reaction processes can lead to the noncoincidence of primary and secondary adsorption runs.

### 3. Results and Discussion

**3.1. Adsorption Microcalorimetry.** Figure 1a shows the 303 K volumetric adsorption isotherms of CO on G573, G673, and G773, while Figure 1b shows the corresponding calorimetric isotherms. Experimental points relative to the secondary adsorption isotherms (open symbols) are reported only in Figure 1a, and only for the first two activation temperatures, since in all other cases (i.e., CO amounts adsorbed on G773, and adsorption heats evolved from all samples) the secondary and primary runs were found to coincide. This indicates that the ambient temperature adsorption of CO on  $\gamma$ -Ga<sub>2</sub>O<sub>3</sub> is, as expected, a reversible process (and this aspect will be later confirmed by IR data) in the sense that only for the adsorbed amounts, which are affected by a larger experimental error than adsorption heats, and only for low-temperature samples characterized by a very low adsorbing capacity, there is a marginal and random deviation between primary and secondary runs.

Inspection of Figure 1a,b shows the following main points. (i) CO amounts adsorbed at 303 K are very small,

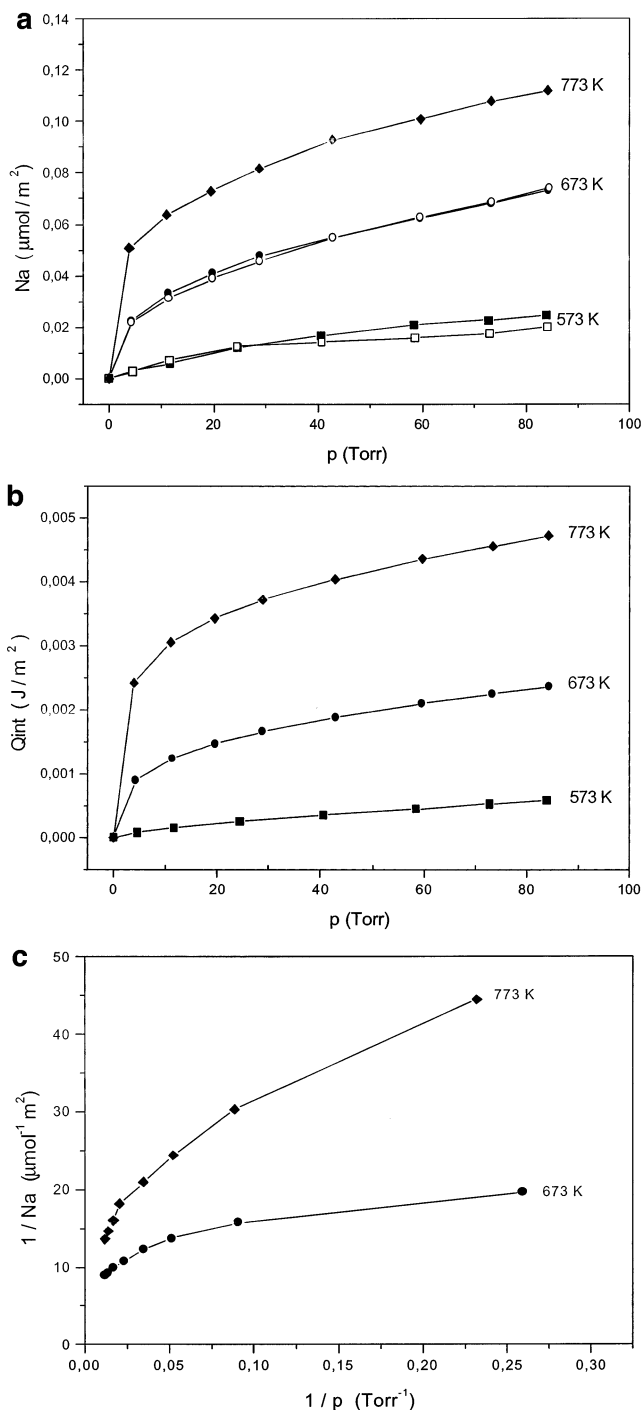


**Figure 1.** (a) Volumetric isotherms of CO adsorption at 303 K on  $\gamma$ -Ga<sub>2</sub>O<sub>3</sub> activated for 4 h at 573 K (G573), 673 K (G673), and 773 K (G773). Open symbols correspond to secondary adsorption runs. (b) Calorimetric CO adsorption isotherms at 303 K for samples G573, G673, and G773. (c) Langmuir type plot of the primary CO adsorption isotherms on samples G673 and G773.

as also found usually for most non-*d* oxides in which CO uptake at ambient temperature can reveal only the strongest fraction(s) of Lewis acid sites.<sup>8</sup> Assuming for oxygen in the spinel-type structure a close-packed arrangement (i.e., a radius of 0.146 nm for surface oxygen ions, corresponding to  $\sim 14.8$  oxygen ions per nm<sup>2</sup>) and assuming for an average and undefined crystal plane of  $\gamma$ -Ga<sub>2</sub>O<sub>3</sub> the Ga<sub>2</sub>O<sub>3</sub> stoichiometry to be maintained (for a

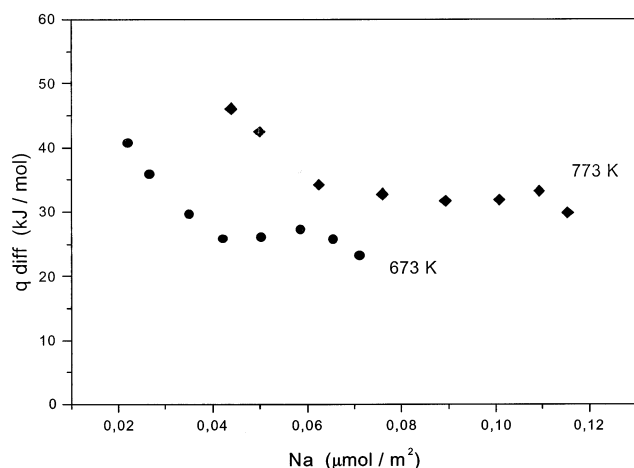


**Figure 2.** Differential heats of adsorption, as a function of CO adsorbed amounts, on G673 and G773. Data refer to the primary adsorption runs.

similar gross calculation on alumina see, e.g., Morterra et al.<sup>9</sup>), it turns out that the maximum CO uptake observed at 303 K for G773 ( $\sim 0.12 \mu\text{mol m}^{-2}$ , or  $\sim 0.07$  molecules per  $\text{nm}^2$ ) hardly reaches about 1% of a statistical monolayer. (ii) The maximum amount of CO adsorbed at 303 K on the various samples, represented by the asymptotic branch of the various adsorption isotherms, increases fast with increasing activation temperature. This indicates that even for relatively mild activation conditions such as those adopted here, the dehydration process brings about a fast formation of  $\text{Ga}^{3+}$  centers having strong Lewis acidity (i.e., highly uncoordinated and thus sufficiently acidic to bind CO at ambient temperature). Note that the onset of a sintering process, leading to an appreciable decrease of surface area (as reported in Table 1), does not affect the area-normalized data of Figure 1, although the overall adsorbed amounts (per unit mass) decrease appreciably. (iii) The overall CO adsorption process is fully reversible, and therefore the type I isotherms<sup>10</sup> cannot indicate whether one or more CO adspecies are formed. For this reason, in situ IR spectroscopy of CO uptake will be resorted to in the next section. If a Langmuir plot is attempted, as shown in Figure 1c where the reciprocal of the adsorbed amount is reported as a function of the reciprocal of the equilibrium CO pressure, it can be seen that no linear correlation is obtained. This indicates that the adsorption phenomenon is heterogeneous, either in terms of the adsorption sites involved or of the relevant molar adsorption heats, or both.

Figure 2 reports the differential adsorption heats ( $-q^{\text{diff}}$ ) as a function of adsorbed amounts for G673 and G773, whereas no  $q^{\text{diff}}$  values are reported for the low-temperature G573 sample, because the scattering of the corresponding data was found to be too high. The widely different adsorbing capacities of the two specimens are monitored by the different abscissa extensions of the two plots. In both cases examined, the  $q^{\text{diff}}$  curve presents two distinctly separated regions, the first of which (related to lower coverages) shows a gradual and quasi-linear decrease of the molar adsorption heats whereas the other one (related to higher coverages) implies virtually constant molar adsorption heats. This observation confirms that the CO adsorption process is a rather heterogeneous one, as already suggested by the Langmuir plots of Figure 1c.

Within this heterogeneous adsorption process, there is a first and more energetic species that turns out to be heterogeneous per se ( $-q^{\text{diff}}$  figures ranging between some 40–45 and some 25–35  $\text{kJ mol}^{-1}$ ) and a second and less energetic species that turns out to be rather homogeneous ( $-q^{\text{diff}} \approx 25\text{--}30 \text{ kJ mol}^{-1}$ ). In either case, and for both samples examined, the molar adsorption heats are compatible with a weak and reversible adsorption process, involving a polarization of the CO molecule at coordinatively unsaturated (cus) surface cationic sites (i.e., weak Lewis acid–base interactions), as usually reported for the ambient temperature adsorption of CO on many non- $\text{d}$  oxidic systems. Note that the data of Figure 2 (and, in particular, the final  $-q^{\text{diff}}$  value virtually constant at  $\sim 25\text{--}30 \text{ kJ mol}^{-1}$ ) tend to exclude the presence, at the surface of  $\gamma$ -Ga<sub>2</sub>O<sub>3</sub> activated at relatively low temperatures, of endothermic surface reconstruction phenomena simulating very low CO adsorption heats, as observed for instance in the case of CO adsorption on some transition aluminas.<sup>8</sup>

**3.2. FTIR Spectroscopy.** To reproduce, on a spectroscopic ground, the ambient temperature adsorption/desorption runs previously carried out with the microcalorimetric/gas-volumetric apparatus, optical adsorption isotherms were obtained by running in situ IR spectra of CO adsorbed under increasing CO pressures (up to a final pressure of  $\sim 100$  Torr) on all  $\gamma$ -Ga<sub>2</sub>O<sub>3</sub> samples prepared as described in the Experimental Section. After the adsorption runs, the samples were evacuated at BT, and the IR spectra confirmed that no detectable absorption bands remained (in any spectral range) for  $p_{\text{CO}} < 10^{-2}$  Torr, as already indicated by the virtual coincidence of primary and secondary adsorption isotherms dealt with in the previous section.

Figure 3 reports, as an example, the IR spectroscopic pattern obtained upon CO adsorption on the sample G673. CO uptake at BT brings about the appearance of appreciable absorptions only in the  $2250\text{--}2150 \text{ cm}^{-1}$  spectral range, indicating that only a weak interaction with surface cus cationic sites is involved in the adsorption process. Still, as expected on the basis of the quantitative and energetic data dealt with in the previous section, the overall IR absorption of adsorbed CO turns out to be rather complex: it is made up of two asymmetrical IR bands of rather different intensities, centered at  $2225\text{--}2210$  and  $2195\text{--}2185 \text{ cm}^{-1}$ , respectively. This confirms, for the strong Lewis acidity of  $\gamma$ -Ga<sub>2</sub>O<sub>3</sub>, a vast site heterogeneity. Also, the pressure dependence of the two bands is quite different. The high-frequency component, being formed first (i.e., at lower CO pressures, when the other component is still virtually absent), becomes broader and broader on the low-frequency side with increasing CO pressure, reaching saturation at still relatively low coverages. Unlike that, the low-frequency component ( $2195\text{--}2185 \text{ cm}^{-1}$ ) starts forming at relatively high CO pressure and does not seem to be approaching saturation for a CO pressure as high as  $\sim 100$  Torr.

The two broad and complex bands can be assigned to CO adsorbed on two different families of Lewis acid centers.<sup>3</sup> On the basis of similar assignments reported in the literature for CO adsorbed on active alumina<sup>11,12</sup> and of the spectroscopic behavior of the two bands as a function of activation/calcination temperature (to be described below), we ascribe the band at  $2230\text{--}2210 \text{ cm}^{-1}$  to the C–O stretching mode of CO adsorbed on (different types of) cus  $\text{Ga}^{3+}$  ions located in defective crystallographic sites,

(9) Morterra, C.; Chiorino, A.; Ghiotti, G.; Garrone, E. *J. Chem. Soc., Faraday Trans. 1* **1979**, 75, 271.

(10) Brunauer, S.; Deming, L. S.; Deming, W. S.; Teller, E. *J. Am. Chem. Soc.* **1940**, 62, 1723.

(11) Marchese, L.; Bordiga, S.; Coluccia, S.; Martra, G.; Zecchina, A. *J. Chem. Soc., Faraday Trans.* **1993**, 89, 3483.

(12) Zecchina, A.; Scarano, D.; Bordiga, S.; Ricchiardi, G.; Spoto, G.; Geobaldo, F. *Catal. Today* **1996**, 27, 403.



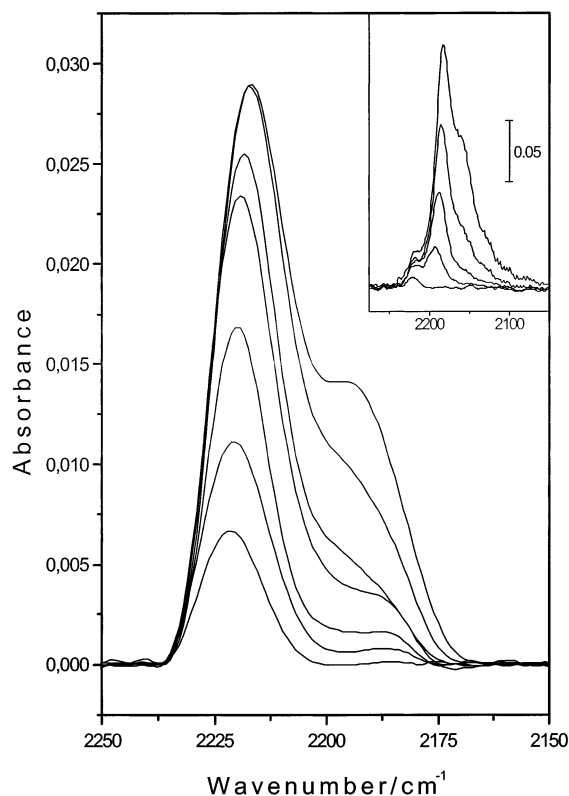


**Figure 3.** Absorbance IR spectra of CO adsorbed, at beam-temperature, on G673. Increasing CO equilibrium pressures ranged from 1 to 100 Torr. The roto-vibrational components due to CO gas were interactively subtracted from the spectra. Inset: Absorbance IR spectra of CO adsorbed at  $\sim 77$  K on the same G673 sample (equilibrium CO pressures from  $10^{-1}$  to 10 Torr).

such as edges and corners of small crystals and/or portions of high-index crystal planes exposed within the mesopores of the system. The band centered at  $2195\text{--}2185\text{ cm}^{-1}$  is assigned to the C–O stretching mode of weak  $\text{Ga}^{3+}\cdots\text{CO}$  adducts formed at cus tetrahedral  $\text{Ga}^{3+}$  ions, which appear in extended (regular) low-index surfaces. The *regular* nature of the sites responsible for the low-frequency band is in apparent contradiction with the low intensity of this band, and this is due to the intrinsic weakness of the adducts formed (i.e., to the low degree of coordinative unsaturation of the sites involved). This implies that on regular low-index crystal planes, only few cus cationic sites possess a sufficient Lewis acidity to coordinate CO at BT. In fact, if we compare the spectra of Figure 3 with those obtained<sup>3</sup> upon CO adsorption on G673 at  $\sim 77$  K (partly reported in the inset to Figure 3), it is seen that at a low temperature the overall amount of CO adsorbed is much higher, as expected of an exothermic process, and that the high-frequency band ( $\sim 2225\text{ cm}^{-1}$ ) has about the same intensity as it has at BT, whereas the low-frequency band ( $\sim 2195\text{ cm}^{-1}$ ) is dominant. At 77 K, also a third band can be observed at  $\sim 2160\text{ cm}^{-1}$ ; this band which does not appear at BT can be ascribed to CO H-bonded to some residual surface OH groups, as described elsewhere.<sup>3</sup> In analogy with what was obtained on transition aluminas,<sup>11,12</sup> part of this low- $\nu$  CO band might be attributable to CO molecules weakly interacting with  $\text{Ga}^{3+}$  cations exhibiting an octahedral incomplete coordination.

When  $\gamma\text{-Ga}_2\text{O}_3$  is activated/calcined at different temperatures, the material undergoes some textural changes (Table 1). These changes are expected to affect to some extent the spectral features of adsorbed CO. This is illustrated in Figure 4, which shows IR spectra corre-

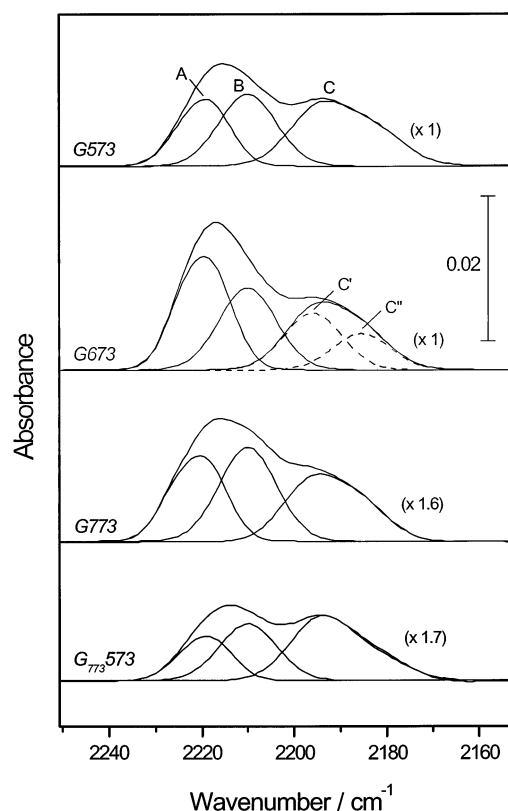


**Figure 4.** Absorbance IR spectra of 100 Torr CO adsorbed at beam-temperature on G573, G673, G773, and  $\text{G}_{773}573$ . The roto-vibrational components due to CO gas were interactively subtracted from the spectra. Individual curves show some of the results of a spectral deconvolution carried out in the  $2250\text{--}2150\text{ cm}^{-1}$  range, following the conditions reported in the text.

sponding to the uptake at BT of 100 Torr CO on the samples G573, G673 (the highest curve of Figure 3), G773, and  $\text{G}_{773}573$ , respectively. To better appreciate the relative intensity of the various spectral components, the curves have been plotted with the low-frequency band ( $2200\text{--}2180\text{ cm}^{-1}$ ) at approximately constant maximum intensity, and the relevant normalizing factors used are reported on the right-hand side of the plots. A spectral deconvolution of the bands has been also carried out, and the results are shown in Figure 4. The following conditions were imposed: (i) The starting point for the first simulation was the spectrum of G673 (see the middle spectrum of Figure 3), for which the combined effect of dehydration degree (relatively high activation temperature) and of surface area (relatively low calcination temperature) yields the strongest and thus best observed spectra. (ii) The spectral simulation of the G673 curve was attained using the minimum necessary number of mixed Gaussian–Lorentzian curves and imposing for the half-bandwidth of the resulting components differences not exceeding 10%. (iii) As a second (and last) step, all other curves were resolved imposing the same number of components obtained for G673 and keeping the frequency of the peak maxima and the half-bandwidth within values not differing from those of G673 by more than 5%. The resulting simulations are satisfactory and indicate that both CO bands can be resolved using only two components for each having largely prevalent Gaussian character. This suggests that also the resolved components are still heterogeneous in nature. The two components of the high-frequency band have been termed A and B, whereas for the low-frequency band only the symbol C was adopted, even if band C is also made

**Table 2. Surface-Area-Normalized Integral Absorbance of CO Components (cm<sup>-1</sup> m<sup>-2</sup>): Adsorption at BT, under a CO Pressure of 100 Torr**

sample	A, 2225–2218 cm <sup>-1</sup>	B, 2210 cm <sup>-1</sup>	A + B, 2225–2210 cm <sup>-1</sup>	C, 2195–2185 cm <sup>-1</sup>	(A + B)/C	A/C
G573	0.077	0.095	0.172	0.124	1.4	0.6
G673	0.136	0.107	0.243	0.122	2.0	1.1
G773	0.081	0.104	0.185	0.103	1.8	0.8
G <sub>773</sub> 573	0.036	0.099	0.135	0.090	1.5	0.4

up of two components (C' and C''), as shown in Figure 4 for the starting spectrum G673.

Table 2 reports the normalized integral absorbance (absorbance units per unit surface area, that is, normalized against sample weight and specific surface area) of the resolved components obtained for the various samples examined, and some ratios therefrom. Two main points can be noted. (i) On passing from G573 to G673 (with no change of specific surface area, as shown in Table 1), the intensity of the low-frequency band C does not change, and this suggests that the family of surface Lewis acid sites located in regular positions tends to acquire its maximum concentration in the early stages of the activation process. Unlike that, the intensity of the high-frequency band increases appreciably following the surface dehydroxylation process, and this is particularly evident for the A component absorbing at the highest frequency, which is due to sites characterized by the highest unsaturation. All this seems reasonable, but a first contradictory aspect appears when comparing G573 with G673. The overall normalized absorbance (A + B + C) passes from 0.30 to 0.37 (with an increase of some 20–25%), whereas the maximum uptake indicated by the isotherms G573 and G673 of Figure 1a passes from  $\sim 0.02$  to  $\sim 0.06$   $\mu\text{mol m}^{-2}$ , corresponding to an increase of some 200%. Consider that the use of overall normalized absorbances (A + B + C), to be compared with overall normalized adsorbed amounts from gas-volumetric measurements, implies not that all species exhibit the same molar extinction coefficient ( $\epsilon$ ) but that each individual species maintains its own  $\epsilon$  on varying the sample treatment conditions. And this assumption turns out to be not realistic. (ii) On passing from G673 to G773 (with a  $\sim 10$ – $15\%$  decline of surface area, as shown in Table 1), the normalized intensity of both CO band profiles is observed to decline by some 20%. This spectroscopic result would suggest that the overall surface concentration of Lewis acid sites is affected more by the incipient sintering process than by the higher dehydroxylation degree reached. This indication is even more contradictory than the one reported above, as the isotherms G673 and G773 of Figure 1a clearly show that the maximum CO uptake (i.e., the maximum specific adsorption capacity) does not decline but increases again by a factor of  $\sim 2$  (maximum CO uptake from  $\sim 0.06$  to  $\sim 0.11$   $\mu\text{mol m}^{-2}$ ).

It is thus deduced that no reliable information with an absolute quantitative meaning can be obtained from IR spectroscopic data, at least for the case of the CO/ $\gamma$ -Ga<sub>2</sub>O<sub>3</sub> system. At least two reasons can be thought to contribute to the observed lack of correspondence between gas-volumetric quantitative data and IR intensity data:

(i) The temperature of the samples in the IR beam (BT) does not correspond to the temperature of the samples in the calorimetric cell. In particular, BT being certainly higher than 303 K, it is quite likely that the amount of the weakly adsorbed species C is largely underestimated by the spectroscopic measurement. Still, this only effect (certainly present) cannot explain the dramatically different trend exhibited by spectroscopic and gas-volumetric adsorption measurements, since the probable artifact

relative to the intensity of the band profile C should affect all adsorption isotherms.

(ii) For reasons that are likely to be connected with the high light scattering of the  $\gamma$ -Ga<sub>2</sub>O<sub>3</sub> sample and with its sintering rate upon increasing calcination temperature, the usual (and convenient) assumption of the validity of the Beer–Lambert equation for heterogeneous systems turns out to be particularly wrong. This delicate problem of applied spectroscopy has been recently dealt with at length<sup>13</sup> for another heterogeneous system: the methanol/silica system. Even when in several other cases of CO adsorption on oxidic systems the use of the Beer–Lambert equation led to reasonable results,<sup>14–16</sup> the present CO/ $\gamma$ -Ga<sub>2</sub>O<sub>3</sub> system confirms the recent conclusion<sup>13</sup> that the use of the concept of molar absorption coefficients for adsorbed species is per se questionable and risky.

Going back to the normalized absorbance data of Table 2, it is possible that they can lead to some reliable conclusions if they are used only in relative terms. For instance, on passing from G673 to G773, it can be observed that the (artifact) decline of the high-frequency band (A + B) is larger than the (artifact) decline of the low-frequency band C: the (A + B)/C ratio goes from 2.0 to 1.8, and within the high-frequency band (A + B), the component A declines most, so that the A/C ratio goes from 1.1 to 0.8. This observation, which is based on the relative intensity of the spectral components in each spectrum, is probably reliable. It is certainly consistent with the proposed assignment of the high-frequency band to CO adsorbed on defective Lewis acid sites, as defective crystal terminations are bound to be affected by sintering processes much more than sites located in regular crystal terminations. Moreover, the trend just discussed for G673–G773 is confirmed by the last sample examined (G<sub>773</sub>573): when the mildly sintered G773 sample is rehydrated and then further dehydrated at 573 K, the band intensity ratios do not recover the values they had after the first activation at 573 K (G573) and, in particular, the A/C ratio (passing from 0.6 to 0.4) reveals an irreversible decrease of the most defective family of  $\text{Ga}^{3+}$  sites, caused by the calcination step at 773 K.

#### 4. Conclusions

The  $\gamma$ -Ga<sub>2</sub>O<sub>3</sub> polymorph was found to possess strong Lewis acidity, as revealed by CO adsorption at ambient temperature. However, the surface concentration of active sites turned out to be rather low.

The CO/ $\gamma$ -Ga<sub>2</sub>O<sub>3</sub> system is a rather heterogeneous one. The reversible CO adsorption process does not follow the Langmuir equation, and several types of  $\text{Ga}^{3+}$  surface sites were revealed by the use of vibrational spectroscopy. These various types of coordinatively unsaturated  $\text{Ga}^{3+}$  ions can be grouped together into two main families. One family of strong Lewis sites is related to defective crystallographic

(13) Morterra, C.; Magnacca, G.; Bolis, V. *Catal. Today* **2001**, *70*, 43.

(14) Bolis, V.; Fubini, B.; Garrone, E.; Morterra, C.; Ugliengo, P. *J. Chem. Soc., Faraday Trans.* **1992**, *88*, 391.

(15) Bolis, V.; Morterra, C.; Fubini, B.; Ugliengo, P.; Garrone, E. *Langmuir* **1993**, *9*, 1521.

(16) Morterra, C.; Bolis, V.; Magnacca, G. *Langmuir* **1994**, *10*, 1812.

structures, whereas the second family, scarcely active at ambient temperature but much more active at low temperatures, is related to regular crystallographic sites (e.g., extended patches of low-index crystal planes). Lewis acid sites of the former family are observed to undergo an appreciable decline as soon as thermal treatments at  $T \geq 700$  K bring about the onset of a sintering process.

The combined use of in situ IR spectroscopy and adsorption microcalorimetry has been found to be very useful in order to understand the detailed qualitative nature of the adsorption process as well as the overall quantitative and energetic aspects of this process. However, unlike some other adsorbent/adsorbate systems, the

quantitative (i.e., absolute intensity) aspects of the IR spectroscopic data turn out to be rather misleading; on going from one sample to another, molar absorption coefficients, a fundamental parameter proposed for homogeneous systems, were not found to keep constant values.

**Acknowledgment.** This study was partly financed with funds from MURST (COFIN 2000, section 03). M.R.D. thanks the Spanish Ministry of Education for a Ph.D. fellowship.

LA026362X